Geophysical Research Letters

RESEARCH LETTER
10.1029/2019GL082740

Abyssal Transport Variations in the Southwest South Atlantic: First Insights From a Long-Term Observation Array at 34.5°S

Daniel Valla[1,2,3], Alberto R. Piola[1,2,3], Christopher S. Meinen[4], and Edmo Campos[5,6]

[1]Departamento Oceanografía, Servicio de Hidrografía Naval, Buenos Aires, Argentina, [2]Departamento Ciencias de la Atmósfera y los Océanos, Facultad de Ciencias Exactas y Naturales, Universidad de Buenos Aires, Buenos Aires, Argentina, [3]UMI/IFAECI, CONICET, Buenos Aires, Argentina, [4]Atlantic Oceanographic and Meteorological Laboratory, Miami, FL, USA, [5]Instituto Oceanográfico, Universidade de São Paulo, São Paulo, Brazil, [6]Gulf Environments Research Institute, American University of Sharjah, Sharjah, United Arab Emirates

Key Points:
- The abyssal flow is strongly variable, and its time variations greatly exceed the time mean
- The meridional absolute volume transport in the abyssal layers is driven by bottom pressure changes taking place away from the western margin
- The abyssal transport contributes significantly to the time variability of the Deep Western Boundary Current

Supporting Information:
- Supporting Information S1

Correspondence to:
D. Valla,
dvalla@hidro.gov.ar

Citation:
Valla, D., Piola, A. R., Meinen, C. S., & Campos, E. (2019). Abyssal transport variations in the southwest South Atlantic: First insights from a long-term observation array at 34.5°S. *Geophysical Research Letters*, *46*. https://doi.org/10.1029/2019GL082740

Received 7 MAR 2019
Accepted 13 MAY 2019
Accepted article online 20 MAY 2019

Abstract The zonal structure and time variability of the abyssal flow (below 3,000 dbar) in the South Atlantic western boundary is investigated using a combination of moored observations and simultaneous hydrographic/velocity sections at 34.5°S during 2009–2018. Moored direct velocity measurements near the bottom show strong variability with a peak-to-peak range exceeding 80 cm/s and dominant signals at times scales of 1–2 months. Daily time series of the meridional absolute geostrophic volume transport computed from the moorings reveals a highly energetic record with a temporal standard deviation of 8.3 Sv and peak-to-peak variations of 49 Sv, suggesting a significant contribution of the abyssal layer flows to the Deep Western Boundary Current time variability. The absolute transport is mostly driven by barotropic changes that are dominated by variations in the bottom pressure ~650 km away from the continental slope.

Plain Language Summary The coldest, densest waters of the world's oceans sink near Antarctica to depths greater than 3,000 m and flow into other basins along the complex seafloor of the abyss. These waters play a key role in redistributing heat and carbon throughout the globe on time scales of centuries to millennia and therefore have a profound impact on the Earth's climate. The gateway northward into the Atlantic Ocean is along the western edge of the South Atlantic. This study presents 9 years of unprecedented, continuous observations of the abyssal flow across 34.5°S off the South American coast together with deep current velocity measurements collected during eight oceanographic cruises in the region since 2009. By combining these observations, we provide a general picture of the abyssal circulation in the region and show that, rather than being slowly changing, it rapidly and strongly varies on time scales as short as 1–2 months.

1. Introduction

The Atlantic Meridional Overturning Circulation (AMOC) is largely responsible for transporting mass, heat, and salt, all quantities that have a critical impact on regional and global climate (e.g., Buckley & Marshall, 2016 ; Rahmstorf et al., 2015, and references therein). Most studies of AMOC time variability to date have focused on the upper cell, characterized by southward flow of relatively cold waters that sink in the high-latitude North Atlantic and a return northward transport of relatively warm waters in the upper/intermediate levels. In reality, however, the AMOC also involves a deeper cell that is comprised of an abyssal limb that conveys very dense waters that originate near Antarctica to the north, where they upwell and mix into lighter waters that return to the south at middepths adjacent to the southward flow of the upper AMOC cell (e.g., Lumpkin & Speer, 2007). This abyssal cell is quite weak in the North Atlantic (e.g., ~1 Sv; Frajka-Williams et al., 2011); however, in the South Atlantic, this is of nearly equal strength as the upper cell (e.g., Lumpkin & Speer, 2007). Estimates based on inverse techniques indicate that as much as 5.6 ± 3.0 Sv are transported across 32°S by the abyssal limb, about 45% of the total estimated overturning at this latitude derived from a transatlantic hydrographic section (Lumpkin & Speer, 2007) and almost 40% of the total upper cell overturning estimates across 34.5°S derived from continuous in situ time series observations and Expendable bathythermograph sections (Meinen et al., 2018).

Topographic blocking, that is, the existence of the Walvis Ridge, severely limits north-south abyssal layer exchanges in the Cape Basin east of the Mid-Atlantic Ridge (e.g., Mantyla & Reid, 1983). As a result, the abyssal AMOC cell flows are largely confined west of the Mid-Atlantic Ridge. The deeper limb of the

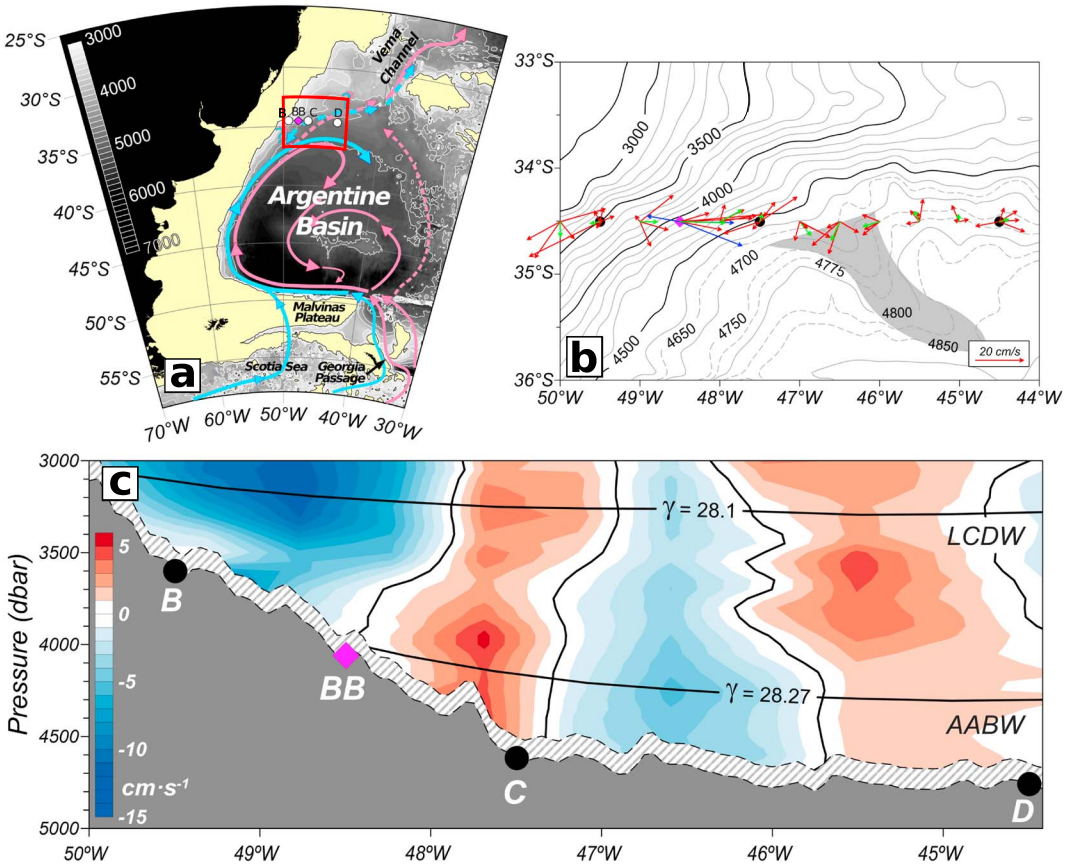

Figure 1. (a) Schematic diagram of the abyssal circulation in the southwest South Atlantic. The light blue and pink paths represent the flow at the LCDW and AABW levels, respectively (dashed paths indicate unconfirmed pathways). The red box indicates the domain shown in (b). (b) Vertically averaged bottom-track measurements (collected in the deepest ~120 m of the water column) from LADCP casts collected between 2011 and 2018 (red arrows; note that LADCP data was not collected at all locations during every section). The green arrows are the averages of all of the velocities collected at each location, and the blue arrows at 48.5°W identify LADCP casts collected simultaneously with the current meter measurements at Site BB (shown in Figure 2). The shaded region indicates the location of an elongated elevation extending south of the array as discussed in the text. (c) Average section of meridional velocity computed from eight LADCP sections occupied between 2011 and 2018. The solid lines indicate the average neutral density (γ) surfaces used to delimit the water masses. The circles (diamonds) in all panels are the locations of the pressure-equipped inverted echo sounder (current- and pressure-equipped inverted echo sounders) along the mooring array. The name convention for the sites is chosen accordingly with previous studies in the region. Contours in (a) and (b) are the bottom topography from The General Bathymetric Chart of the Oceans (GEBCO; IOC et al., 2003). AABW = Antarctic bottom water; LADCP = lowered acoustic Doppler current profiler; LCDW = Lower Circumpolar Deep Water.

abyssal AMOC cell is fed by two distinct water masses. The densest bottom waters originate in the Weddell Sea and leak into the Argentine Basin through deep passages east of the Scotia Sea (Georgi, 1981; Naveira Garabato et al., 2002). Away from their source, these waters are commonly referred to as Antarctic Bottom Waters (AABW; Figure 1a). The second component is a dense variety of the oxygen-poor, recirculated waters flowing around Antarctica within the Antarctic Circumpolar Current, identified as Lower Circumpolar Deep Water (LCDW). The LCDW enters the Argentine Basin over the Malvinas Plateau and east of the South Georgia Island, joining the AABW, and flows northward along the west margin of the Argentine Basin as a western boundary current (Figure 1a; Naveira Garabato et al., 2002). Although the mean circulation in the vicinity of 35°S is not yet well determined, a fraction of the AABW eventually leaks into the Brazil Basin through the Vema and Hunter channels (Hogg et al., 1982; Zenk et al., 1999). A number of secondary pathways for AABW in the interior of the Argentine Basin have also been proposed on the basis of hydrographic measurements (Coles et al., 1996; Georgi, 1981). By contrast, hydrographic measurements collected at different latitudes along the western boundary of the South Atlantic show only sporadic presence of LCDW north of 34.5°S and west of 30°W (Valla et al., 2018).

Previous efforts to monitor the abyssal MOC cell in the southwest South Atlantic have mainly focused in measuring the AABW flow between the Argentine and Brazil basins through the narrow Vema and

Hunter channels. On a broader scale, however, the volume transport associated with the abyssal limb in the South Atlantic is poorly understood. The purpose of this study is to characterize the abyssal flows in the northwest Argentine Basin at 34.5°S using a combination of nearly 10 years of continuous observations of volume transports derived from a pressure-equipped inverted echo sounder (PIES) array, 4 years of continuous, near-bottom direct velocity observations, and snapshot direct velocity measurements collected during eight cruises occupied along a repeated hydrographic section.

2. Data and Methods

In March 2009, an array of four PIES was deployed at 34.5°S between 51.5°W (~1,300 m) and 44.5°W (~4,700 m) to measure the meridional flow at the western boundary (e.g., Meinen et al., 2012). Two additional current- and pressure-equipped inverted echo sounders (CPIESs), which include a single-point current meter 50 m above the ocean bottom, were added to the array in December 2012. In this paper, measurements from the four easternmost instruments (three PIES and one CPIES located at depths greater than 3,500 m, Figure 1a) are used to characterize the abyssal flow near the western boundary. The travel time data collected hourly by the PIES/CPIES are used to estimate continuous full water column profiles of temperature, salinity, and density at each mooring site via the Gravest Empirical Mode (GEM) method (Meinen & Watts, 2000). These profiles are then combined with the measured bottom pressure data to derive continuous times series of full water column profiles of absolute meridional geostrophic velocity between each pair of instruments (e.g., between sites B-BB, BB-C, and C-D; see, e.g., Meinen et al., 2017, for more details). Note that due to the well-known leveling problem (e.g., Donohue et al., 2010), the bottom pressure differences only provide estimates of the barotropic flow variability and not the time mean (e.g., Meinen et al., 2012). For this study, a time mean barotropic velocity between each pair of PIES/CPIES sites, was added based on the time mean of a 35-year run of the Ocean For the Earth Simulator (OFES) numerical model (Masumoto et al., 2004; Sasaki et al., 2008). Following Meinen et al. (2017), constant velocities of 0.13, 0.66, and −0.16 cm/s were added to the daily estimates of the absolute geostrophic velocity full-water profiles between sites B-BB, BB-C, and C-D, respectively, in order to match the time-averaged estimates derived from the PIES at 1,500 dbar to the time-averaged velocity output from OFES at that pressure level. The results presented here are not highly sensitive to the choice of this reference level or the numerical model used as input for the time mean velocities between each pair of instruments.

To estimate the absolute volume transports in the key layers in the abyssal overturning cell, the velocities that were derived as described above are integrated between neutral density surfaces (γ) that define the layer interfaces. The water mass interfaces used herein were $\gamma = 28.10$ kg/m^3 and $\gamma = 28.27$ kg/m^3 for the interfaces between North Atlantic Deep Water and LCDW, and between LCDW and AABW, respectively, following Valla et al. (2018) (e.g., Figure 1c). The transports time series described in this article have been averaged to produce daily values, and the time series have been smoothed with a second-order Butterworth low-pass filter, with a 30-day cutoff period, applied forward and backward to avoid phase shifts.

Together with the deployment of the PIES/CPIES array, a repeated hydrographic section along 34.5°S between the coast and 44.5°W, has been occupied annually/semiannually since 2009. Starting in 2011, direct velocity measurements have also been collected using a TRDI 300-kHz WH Monitor lowered acoustic Doppler current profiler (LADCP) during each conductivity-temperature-depth cast. The LADCP data have been processed with the LDEO_IX version 12 implementation of the velocity inverse method (Visbeck, 2002) in the same fashion detailed by Valla et al. (2018). Eight sections involving LADCP data are available for analysis between July 2011 and October 2018. Due to rough weather conditions, however, LADCP measurements were not collected offshore of 47.5°W during three of these sections. In this study, we also analyze the highly accurate LADCP bottom-track (BT) velocity measurements separately to investigate patterns of the flow in the deepest layer; these data are available in the deepest ~120 m of the water column.

Hourly direct velocity observations made 50 m off the bottom at site BB using a single-point acoustic current meter (~4,100-m depth; see Figure 1a) collected between December 2012 and October 2016 provide an unprecedented ~4-year continuous record of the abyssal flow in the region. These direct velocity data were smoothed with a second-order Butterworth low-pass filter (30-day cutoff period) applied forward and backward to avoid phase shifts for the analysis.

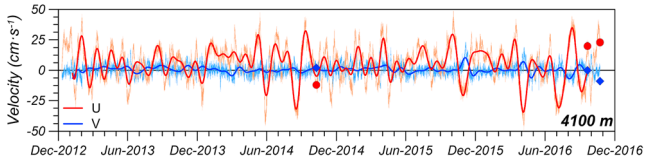

Figure 2. Zonal (*U*, red) and meridional (*V*, blue) hourly velocity records at 4,100-m depth at Site BB (48.5°W; thin lines). Also shown are the low-pass-filtered records using a 30-day cutoff period (thick lines). Red circles (blue diamonds) are the zonal (meridional) component of the vertically averaged velocity determined from bottom-track measurements during three concurrent lowered acoustic Doppler current profiler casts (September 2014, September 2016, and October 2016).

3. Results and Discussion

3.1. The Abyssal Flow

The zonal and vertical structure of the abyssal meridional flow as depicted by the average of the LADCP sections is presented in Figure 1c. West of ~48°W, the LCDW flows southward with relatively stronger velocities (>5 cm/s) in the upper portion of the layer. This suggests an influence of the Deep Western Boundary Current (DWBC), which flows southward west of ~49°W (Meinen et al., 2012, 2017; Valla et al., 2018). East of 48°W the section shows two northward jets centered at ~47.5°W and ~45.5°W and a relatively weak southward flow between ~46° and 47°W. The southward flow is deeper than 2,800 dbar and intensifies toward the bottom. The vertically averaged BT measurements, which have a higher accuracy than the standard LADCP data, also exhibit this pattern for the near-bottom flow (Figure 1b). This zonal structure with relatively weak, successive northward and southward jets east of ~49°W is also observed in a 5-year (2009–2014) average section of the meridional flow derived from the OFES model presented by Meinen et al. (2017). Perhaps more interestingly, our BT measurements also indicate that the AABW flows southward in this portion of the section, that is, toward its formation region. This result is in agreement with Meinen et al. (2017), who also found AABW propagating on average southward between sites C and D on the basis of 2 years (2012–2014) of PIES data. Those authors highlight that this counter intuitive result implies a possible alternative pathway through which AABW would flow counterclockwise along the eastern margin of the Argentine Basin and would reach the array from north of 34.5°S. The existence of such a pathway has also been speculated by Coles et al. (1996) on the basis of abyssal tracer and hydrographic measurements. By contrast, no evidence for this has been found from recent water mass analyses (Valla et al., 2018). Our BT measurements suggests that, at least based on the average of five ship sections, the southward flow is localized at 47–46°W and colocated over a NW-SE oriented elongated elevation south of 34.5°S and east of 47°W (shaded region in Figure 1b). This may imply a small-scale circulation steered by the local topography and may explain the southward flow of AABW at this location. It is clear that given the strongly variable deep flow observed east of site B (e.g., Meinen et al., 2012), it is not yet possible to obtain a conclusive result about the time-averaged flow, which stresses the importance of collecting further deep direct velocity observations in this region.

The abyssal flow can be further analyzed, albeit at a single geographic point, using the 4-year continuous CPIES velocity observations at site BB. The time-average zonal component (*U*) is 1 order of magnitude higher and presents greater standard deviation (5.5 ± 15 cm/s) than the meridional component (*V*, 0.5 ± 4.7 cm/s). The temporal variability greatly exceeds the time mean values for both components, demonstrating the highly variable nature of the flow. The variance at time scales shorter than 40 hr is less than 3% of the total variance, indicating diurnal/semidiurnal tides play only a minor role at this location. The strong variability of the zonal flow associated with longer time scales is depicted by the 30-day low-pass-filtered record, showing a peak-to-peak range of 60 cm/s, while the peak-to-peak range of the unfiltered record is 100 cm/s (Figure 2). The snapshot BT measurements also show a clear prevalence of the zonal flow at this location (Site BB, Figure 1b). The weak meridional flow may also suggest a transition between a southward abyssal flow driven by the DWBC onshore and a northward flow offshore. The CPIES current meter data are in excellent agreement with the three concurrent, vertically averaged, LADCP BT measurements at site BB. The instantaneous differences in *U* and *V* are generally smaller than 3 cm/s (Figure 2). Only one cast, collected in October 2016, shows a large difference in the meridional component (9 cm/s). The power spectrum of the unfiltered, hourly record is presented in the supporting information and shows energy peaks at periods 24, 32, 43, and 72 days, with the highest energy concentrated in periods of 26–52 days (supporting information Figure S1). Previous observations in the Brazil-Malvinas Confluence, just south of the PIES/CPIES array (near 37–38°S) also found significant variability in this frequency band (Garzoli & Simionato, 1990). Those authors ascribed this variability to propagating topographic Rossby Waves.

3.2. Meridional Transport

In this section, we estimate the absolute meridional volume transport in the LCDW and AABW layers using the PIES/CPIES records. The absolute transport consists of the sum of a relative (baroclinic) component

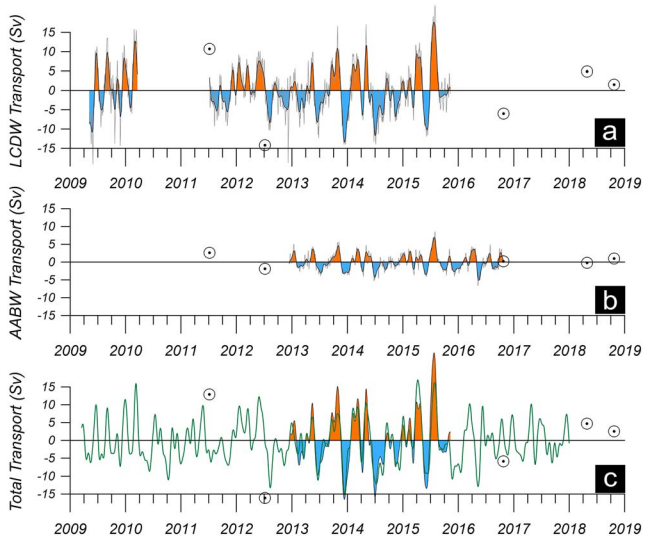

Figure 3. (a, b) Time series of the meridional Lower Circumpolar Deep Water (a) and Antarctic Bottom Waters (b) absolute volume transport. Both the unfiltered daily transports (gray) and the 30-day low-pass-filtered transports (filled) are shown. (c) Time series of the total (LCDW + AABW) meridional absolute volume transport (filled). Superimposed is the proxy for the total transport derived from the pressure record at site D as detailed in the text (green). Both time series are smoothed with a 30-day low-pass filter. The circles in all panels are the corresponding transport estimates derived from simultaneous lowered acoustic Doppler current profiler bottom-track measurements (as detailed in Table 1).

Table 1
Meridional LCDW and AABW Absolute Volume Transports (in Sverdrups) Computed From LADCP Bottom-Track Measurements Collected During Five Hydrographic Cruises Across the Mooring Array (See Figure 1 for Location)

Cruise date	LCDW		AABW		LCDW + AABW	
	LADCP	PIES	LADCP	PIES	LADCP	PIES
July 2011	10.7	2.6	2.6	N/A	12.9	N/A
July 2012	−14.2	1.1	−1.9	N/A	−16.1	N/A
Oct. 2016	−6.0	N/A	0.2	−0.7	−5.9	N/A
Apr. 2018	4.9	N/A	−0.2	N/A	4.7	N/A
Oct. 2018	1.5	N/A	1.0	N/A	2.5	N/A
AVG ± STD	−0.6 ± 9.7	*0.1 ± 5.9*	0.3 ± 1.6	*0.0 ± 2.3*	−0.4 ± 11.0	*0.1 ± 8.2*

Note. Also shown are the concurrent estimates from the colocated PIES measurements. The final row shows the time mean ± standard deviation of the estimates (the PIES statistical estimates, shown in italics, were computed using the full record length instead of the individual estimates corresponding to each hydrographic section). AABW = Antarctic Bottom Waters; LADClowered acoustic Doppler current profiler; LCDW = Lower Circumpolar Deep Water; PIES = pressure-equipped inverted echo sounder.

estimated from the acoustic travel time measurements and the GEM lookup tables and a reference (barotropic) component computed from the pressure measurements made by the instrument (e.g., Meinen et al., 2012). However, the contribution of the relative component is negligible in the abyssal layers due to the weak baroclinicity of the flow. Indeed, the standard deviation of the barotropic component of the meridional transport across the array within the LCDW/AABW layers is 8.4 Sv, with a peak-to-peak range of 46.9 Sv, while the baroclinic component standard deviation is 0.3 Sv and the peak-to-peak range is 1.9 Sv (not shown).

Daily estimates of the meridional LCDW (T_{LCDW}) and AABW (T_{AABW}) absolute transport across the array are depicted in Figures 3a and 3b, respectively. The time series show strong variability in both layers: The standard deviation and peak-to-peak range are 5.9 and 41.0 Sv for T_{LCDW}, respectively, and 2.3 and 15.2 Sv for T_{AABW}. Approximately, 85% of the variance is concentrated at time scales longer than 30 days in both layers. A spectral analysis of T_{LCDW} and T_{AABW} reveals a broad energy maximum at periods of 70 to 190 days, with peaks at 105 and ~170 days (supporting information Figures S2c and S2d). These results are in agreement with findings from Meinen et al. (2017), who also found a significant variance of the DWBC at 34.5°S in this period range using the first 5 years of the PIES/CPIES records utilized herein. Those authors associated the transport variations at these time scales with westward-propagating vortices consistent with Rossby Wave-like features. Interestingly, the power spectra of the now nearly 10-year-long bottom pressure records at each of the four sites involved in the calculation show that only site D presents variability at these time scales (supporting information Figures S2a and S2b). According to these results, the aforementioned features would not dominate the bottom pressure variability well inshore of site D (44.5°W).

The power spectra analysis suggests that bottom pressure variations at site D dominates the variability of the total abyssal transport ($T_{\mathrm{LCDW}} + T_{\mathrm{AABW}}$). Indeed, these two variables present a high linear relationship ($r =$ 0.88, supporting information Figure S3), meaning that almost 80 % of the variability observed in the daily estimates of $T_{\mathrm{LCDW}} + T_{\mathrm{AABW}}$ are explained by variations of the bottom pressure at site D. Here we use a simple linear regression (supporting information Figure S3) to develop a proxy and extend the ~3-year $T_{\mathrm{LCDW}} + T_{\mathrm{AABW}}$ time series to March 2009 to April 2018 (i.e., the full bottom pressure record at site D). The low-pass-filtered time series of $T_{\mathrm{LCDW}} + T_{\mathrm{AABW}}$ together with the low-pass-filtered proxy derived from the linear regression are presented in Figure 3c. The transports estimated directly from the PIES/CPIES measurements exhibit a standard deviation somewhat larger (8.2 Sv) than the proxy (6.5 Sv). Large intraannual variations are observed in both time series (e.g., the transport variation of ~40 Sv between June and August 2015, Figure 3c). By contrast, interannual variability is much smaller: The annual mean transports derived from the proxy have a standard deviation of only 0.8 Sv. This is also observed in the spectral analysis of the ~9-year-length proxy, which shows no significant peaks at periods longer than 100 days (not shown).

LADCP direct velocity observations provide independent estimates of quasi-instantaneous meridional absolute transport in the abyssal layers during the dates of each cruise (Table 1). The BT measurements are used to compute estimates of the absolute transport as follows: For each individual section, the vertically averaged BT meridional velocity at each LADCP station is extrapolated upward to the top of the LCDW layer

(~3,100–3,200 dbar, Figure 1c) by considering a negligible baroclinicty in the velocity field, as discussed above. Finally, the resulting velocity field is integrated from the top of the LCDW layer to the bottom and from sites B to D. Although only three simultaneous estimates between the LADCP snapshots and the PIES/CPIES are available due to gaps in the records, both estimates exhibit a similar standard deviation (Table 1 and Figure 3c). The standard deviation from the five estimates derived from the LADCP is 9.7 Sv for the LCDW layer and 1.6 Sv for the AABW layer, whereas the estimates from the PIES/CPIES transports are 5.9 and 2.3 Sv, respectively. The LADCP estimates also suggest an average southward LCDW (−0.6 Sv) and northward AABW (0.3 Sv) transport across the entire array (Table 1). By contrast, the average LCDW and AABW transports estimated from the PIES measurements are 0.1 and 0.0 Sv, respectively. Note, however, that these estimates strictly depend on the time mean velocities derived from OFES at 1,500 dbar, as explained in section 2. Nevertheless, the very large daily standard deviations, as compared to the time means, observed in both the PIES estimates as well as the LADCP estimates highlights the need for continuous deep ocean observations to ascertain the sense and magnitude of the mean flow. The nearly zonal orientation of the deep isobaths in the vicinity of the zonal array (greater than 4,000 m, Figure 1b) also hinders the estimation of the along-isobath abyssal flow across the array. Ongoing plans for extending the array eastward to the Mid-Atlantic Ridge will enable a more comprehensive observation of the abyssal flow in the northern Argentine Basin.

4. Conclusions

Data from eight LADCP snapshots suggest that the abyssal flow is strongly influenced by the DWBC onshore of ~48°W thus flowing southward on average, while no clear direction of the flow is obtained from these snapshots farther offshore. This is more likely a result of the strong variability in this region, as shown by nearly 4 years of continuous current observations at 4,100 m, which present peak-to-peak variations of ~100 cm/s and an average value of 5.5 cm/s. The absolute volume transport in the LCDW/AABW layer, that is, the abyssal limb of the AMOC at 34.5°S, contributes a significant portion of the transport variability associated with the DWBC at this location. A daily multiyear time series of meridional absolute transport integrated in the LCDW and AABW layers shows a standard deviation of 8.2 Sv with a peak-to-peak range of 49 Sv, as compared to a 22.8-Sv standard deviation associated with the full DWBC (i.e., the complete flow below 800 dbar) reported by Meinen et al. (2017) based on much shorter records. Changes in transport are mainly driven by the barotropic component of the transport, which, in turn, is dominated by bottom pressure variations in the easternmost end of the array, located ~650 km east of the continental slope. The tight correlation between these two quantities was used to derive a 9-year-length proxy of the absolute meridional transport in the LCDW and AABW layers. This time series indicates that the interannual variability of the transport is small (<1 Sv) compared to the intraannual variability and that abyssal flow variations are concentrated on times scales of 100–190 days. This is consistent with the passing of westward-propagating coherent vortices, whereas the current observations at 4,100 m show variability at scales of 26–52 days consistent with topographic Rossby waves crossing the array closer to the western margin of the basin. Uncertainties in a long-term and large-scale characterization of the abyssal flow across 34.5°S are to a large extent due to the strong variability observed both in current records and transport estimates. These results highlight the necessity of continuous observations in order to understand the role of the abyssal limb and its variations in the basin-wide AMOC.

Acknowledgments
Information about obtaining the PIES/CPIES and LADCP data can be found at www.aoml.noaa.gov/phod/SAMOC_international/index.php. We thank the captains and crews of R/V Puerto Deseado and R/V Alpha-Crucis who ably supported our work at sea. This work was financed by the Inter-American Institute for Global Change Research (IAI) grants SGP2076 and CRN3070 (U.S. National Science Foundation grants GEO-0452325 and GEO-1128040) and NOAA Climate Program Office's Ocean Observing and Monitoring Division (FundRef 100007298) under the Southwest Atlantic Meridional Overturning Circulation (SAM) project, with additional support from the NOAA Atlantic Oceanographic and Meteorological Laboratory. The Brazilian component of the research was funded by the São Paulo State Funding Agency (FAPESP, grants 2011/50552-4 and 2017/09659-6). D. Valla was partially supported by a fellowship from CONICET, Argentina. We thank the anonymous reviewers, whose comments on an earlier draft of this manuscript helped improve the final presentation of the results.

References

Buckley, M. W., & Marshall, J. (2016). Observations, inferences, and mechanisms of the Atlantic Meridional Overturning Circulation: A review. *Reviews of Geophysics*, *54*, 5–63. https://doi.org/10.1002/2015RG000493

Coles, V. J., McCartney, M. S., Olson, D. B., & Smethie, W. M. (1996). Changes in Antarctic Bottom Water properties in the western South Atlantic in the late 1980s. *Journal of Geophysical Research*, *101*(C4), 8957–8970. https://doi.org/10.1029/95JC03721

Donohue, K. A., Watts, D. R., Tracey, K. L., Greene, A. D., & Kennelly, M. (2010). Mapping circulation in the Kuroshio extension with an array of current and pressure recording inverted echo sounders. *Journal of Atmospheric and Oceanic Technology*, *27*(3), 507–527. https://doi.org/10.1175/2009JTECHO686.1

Frajka-Williams, E., Cunningham, S. A., Bryden, H., & King, B. A. (2011). Variability of Antarctic Bottom Water at 24.5°N in the Atlantic. *Journal of Geophysical Research*, *116*, C11026. https://doi.org/10.1029/2011JC007168

Garzoli, S., & Simionato, C. (1990). Baroclinic instabilities and forced oscillations in the Brazil/Malvinas confluence front. *Deep Sea Research Part A. Oceanographic Research Papers*, *37*(6), 1053–1074. https://doi.org/10.1016/0198-0149(90)90110-H

Georgi, D. T. (1981). Circulation of bottom waters in the southwestern South Atlantic. *Deep Sea Research Part A. Oceanographic Research Papers*, *28*(9), 959–979. https://doi.org/10.1016/0198-0149(81)90012-1

Hogg, N. G., Biscaye, P., Gardner, W., & Schmitz, W. J. (1982). On the transport and modification of Antarctic Bottom Water in the Vema Channel. *Journal of Marine Research*, *40*, 231–263.

IOC, IHO, and BODC (2003), Centenary edition of the GEBCO digital atlas, edited.

Lumpkin, R., & Speer, K. (2007). Global Ocean Meridional Overturning. *Journal of Physical Oceanography*, *37*(10), 2550–2562. https://doi.org/10.1175/JPO3130.1

Mantyla, A. W., & Reid, J. L. (1983). Abyssal characteristics of the World Ocean waters. *Deep Sea Research Part A. Oceanographic Research Papers*, *30*(8), 805–833. https://doi.org/10.1016/0198-0149(83)90002-X

Masumoto, Y., Sasaki, H., Kagimoto, T., Komori, N., Ishida, A., Sasai, Y., et al. (2004). A fifty-year eddy-resolving simulation of the world ocean—Preliminary outcomes of OFES (OGCM for the Earth Simulator). *Journal of the Earth Simulator*, *1*, 35–56.

Meinen, C. S., Garzoli, S. L., Perez, R. C., Campos, E., Piola, A. R., Chidichimo, M. P., et al. (2017). Characteristics and causes of Deep Western Boundary Current transport variability at 34.5°S during 2009–2014. *Ocean Science*, *13*(1), 175–194. https://doi.org/10.5194/os-13-175-2017

Meinen, C. S., Piola, A. R., Perez, R. C., & Garzoli, S. L. (2012). Deep Western Boundary Current transport variability in the South Atlantic: Preliminary results from a pilot array at 34.5°S. *Ocean Science*, *8*(6), 1041–1054. https://doi.org/10.5194/os-8-1041-2012

Meinen, C. S., Speich, S., Piola, A. R., Ansorge, I., Campos, E., Kersalé, M., et al. (2018). Meridional Overturning Circulation transport variability at 34.5°S during 2009–2017: Baroclinic and barotropic flows and the dueling influence of the boundaries. *Geophysical Research Letters*, *45*, 4180–4188. https://doi.org/10.1029/2018GL077408

Meinen, C. S., & Watts, D. R. (2000). Vertical structure and transport on a transect across the North Atlantic Current near 42°N: Time series and mean. *Journal of Geophysical Research*, *105*(C9), 21,869–21,891. https://doi.org/10.1029/2000JC900097

Naveira Garabato, A. C., Heywood, K. J., & Stevens, D. P. (2002). Modification and pathways of Southern Ocean Deep Waters in the Scotia Sea. *Deep-Sea Research Part I: Oceanographic Research Papers*, *49*(4), 681–705. https://doi.org/10.1016/S0967-0637(01)00071-1

Rahmstorf, S., Box, J. E., Feulner, G., Mann, M. E., Robinson, A., Rutherford, S., & Schaffernicht, E. J. (2015). Exceptional twentieth-century slowdown in Atlantic Ocean overturning circulation. *Nature Climate Change*, *5*(5), 475–480. https://doi.org/10.1038/nclimate2554

Sasaki, H., Nonaka, M., Masumoto, Y., Sasai, Y., Uehara, H., & Sakuma, H. (2008). An eddy-resolving hindcast simulation of the quasi-global ocean from 1950 to 2003 on the Earth simulator. In K. Hamilton, & W. Ohfuchi (Eds.), *High Resolution Numerical Modelling of the Atmosphere and Ocean*, (pp. 157–185). New York, NY: Springer New York. https://doi.org/10.1007/978-0-387-49791-4_10

Valla, D., Piola, A. R., Meinen, C. S., & Campos, E. (2018). Strong mixing and recirculation in the northwestern Argentine basin. *Journal of Geophysical Research: Oceans*, *123*, 4624–4648. https://doi.org/10.1029/2018JC013907

Visbeck, M. (2002). Deep velocity profiling using lowered acoustic Doppler current profilers: Bottom track and inverse solutions. *Journal of Atmospheric and Oceanic Technology*, *19*(5), 794–807. https://doi.org/10.1175/1520-0426(2002)019<0794:DVPULA>2.0.CO;2

Zenk, W., Siedler, G., Lenz, B., & Hogg, N. G. (1999). Antarctic Bottom Water flow through the Hunter Channel. *Journal of Physical Oceanography*, *29*(11), 2785–2801. https://doi.org/10.1175/1520-0485(1999)029<2785:ABWFTT>2.0.CO;2